Molecular Therapy
Nucleic Acids
Original Article

miR-301a-PTEN-AKT Signaling Induces Cardiomyocyte Proliferation and Promotes Cardiac Repair Post-MI

Lixiao Zhen,[1,4] Qian Zhao,[1,4] Jinhui Lü,[1] Shengqiong Deng,[2] Zhen Xu,[1] Lin Zhang,[1] Yuzhen Zhang,[1] Huimin Fan,[1] Xiongwen Chen,[3] Zhongmin Liu,[1] Yuying Gu,[1] and Zuoren Yu[1]

[1]Key Laboratory of Arrhythmias of the Ministry of Education of China, Research Center for Translational Medicine, Shanghai East Hospital, Tongji University School of Medicine, 150 Jimo Road, Shanghai 200120, China; [2]Shanghai Gongli Hospital, The Second Military Medical University, Shanghai, China; [3]Cardiovascular Research Center, Temple University School of Medicine, Philadelphia, PA 19122, USA

Adult hearts are hard to recover after cardiac injury due to the limited proliferative ability of cardiomyocytes. Emerging evidence indicates the induction of cell cycle reentry of cardiomyocytes by special treatment or stimulation, which offers adult heart regenerative potential. Herein, a microRNA (miRNA) screening in cardiomyocytes identified miR-301a enriched specially in the neonatal cardiomyocytes from rats and mice. Overexpression of miR-301a in primary neonatal cardiomyocytes and H9C2 cells induced G_1/S transition of the cell cycle, promoted cellular proliferation, and protected cardiomyocytes against hypoxia-induced apoptosis. Adeno-associated virus (AAV)9-mediated cardiac delivery of miR-301a to the mice model with myocardial infarction (MI) dramatically promoted cardiac repair post-MI *in vivo*. Phosphatase and tensin homolog (PTEN)/phosphatidylinositol 3-kinase (PI3K)/AKT signaling pathway was confirmed to mediate miR-301a-induced cell proliferation in cardiomyocytes. Loss of function of PTEN mimicked the miR-301a-induced phenotype, while gain of function of PTEN attenuated the miR-301a-induced cell proliferation in cardiomyocytes. Application of RG7440, a small molecule inhibitor of AKT, blocked the function of miR-301a in cardiomyocytes. The current study revealed a miRNA signaling in inducing the cell cycle reentry of cardiomyocytes in the injured heart, and it demonstrated the miR-301a/PTEN/AKT signaling as a potential therapeutic target to reconstitute lost cardiomyocytes in mammals.

INTRODUCTION

After heart injury in adults, the regeneration of cardiomyocytes is very limited due to the "terminated" cell proliferative ability and "lack" of cardiac stem cells.[1,2] Myocardial infarction (MI) occurs mostly from coronary artery disease in which heart blood flow is blocked, causing damage to the cardiomyocytes. MI may cause heart failure, heart arrhythmia, cardiogenic shock, or cardiac arrest. There are two potential strategies for restoring the lost cardiomyocytes caused by MI. One is to apply cardiomyocytes differentiated from embryonic stem cells (ESCs) or induced pluripotent stem cells (iPSCs).[3,4] The other is to induce the cell cycle reentry of cardiomyocytes.[5,6]

During heart development, a high rate of the cell cycle activity in cardiomyocytes occurs during fetal life, but the proliferative rate of cardiomyocytes gradually declines during later stages of embryogenesis in mammals.[7] Shortly after birth, most cardiomyocytes exit the cell cycle, becoming "terminally" differentiated cells.[8] Due to the limited rate of cardiomyocyte regeneration responding to injury and stress, most insults ultimately lead to cardiomyocyte hypertrophy or cardiomyocyte dropout induced by necrosis and/or apoptosis.[9–11] Emerging evidence indicates that adult heart may still maintain regenerative potential because of the cell cycle reentry of cardiomyocytes, which promotes cardiomyocyte replacement after injury.[12,13] Although the increased cardiomyocyte cell division is expected after special treatment, the overall effect is still rather limited. As such, developing a new strategy for inducing the cell cycle reentry of cardiomyocytes in the heart is urgently required.

MicroRNAs (miRNAs) are a class of highly conserved small non-coding RNAs regulating the stability or translational efficiency of targeted messenger RNAs through base-pairing interactions mostly within the 3′ untranslated region (UTR).[14] miRNAs have been well demonstrated to regulate diverse biological and pathological processes, including tissue development, cell cycle progression, stem cell self-renewal and differentiation, and tumorigenesis.[15–17]

Several miRNAs, including miRNA-1, miR-133, miR-208, and miR-499, have been reported to be involved in cardiac cell differentiation,

Received 16 February 2020; accepted 25 August 2020;
https://doi.org/10.1016/j.omtn.2020.08.033.

[4]These authors contributed equally to this work.

Correspondence: Zuoren Yu, Key Laboratory of Arrhythmias of the Ministry of Education of China, Research Center for Translational Medicine, Shanghai East Hospital, Tongji University School of Medicine, 150 Jimo Road, Shanghai 200120, China.
E-mail: zuoren.yu@tongji.edu.cn
Correspondence: Yuying Gu, MD, Key Laboratory of Arrhythmias of the Ministry of Education of China, Research Center for Translational Medicine, Shanghai East Hospital, Tongji University School of Medicine, 150 Jimo Road, Shanghai 200120, China.
E-mail: gyy1128@easthospital.cn

cell proliferation, heart development, and cardiac remodeling.[18–20] As the most abundant miRNAs in heart, the miR-1/133a bicistronic clusters are critical regulators of cardiac development. miR-1 can induce cardiac cell differentiation of ESCs both *in vitro* and *in vivo*.[21] Post-MI transplantation with ESCs overexpressing miR-1 significantly enhanced their differentiation into cardiomyocytes.[21] The absence of miR-133a in heart led to ectopic expression of smooth muscle genes and aberrant cardiac cell proliferation. The mice carrying a miR-133a-1/miR-133a-2 double mutation suffered dilated cardiomyopathy and heart failure.[22,23] In addition, miR-15,[24] miR-199a,[6] and the miR-17-92 cluster[25] have been reported to promote cardiomyocyte proliferation *in vitro* and/or *in vivo*.

Our previous study on miRNA screening in cardiomyocytes revealed the enrichment of miR-708 and miR-301a in the heart of neonatal rats and mice.[2,26] miR-708 has been demonstrated to promote differentiation of cardiac progenitor cells and promote cardiac myocyte proliferation.[2,26] However, the function of miR-301a in cardiomyocytes remains unknown.

In the current study, the neonatal cardiomyocyte-enriched miR-301a was demonstrated to induce cell cycle reentry, promote cellular proliferation, and protect cells against hypoxia-induced apoptosis in H9C2 and primary cardiomyocytes. Adeno-associated virus (AAV) 9-mediated cardiac delivery of miR-301a into the mice subjected to MI promoted myocardial regeneration and cardiac repair *in vivo*. The phosphatase and tensin homolog (PTEN)/AKT/cyclin D1 pathway was proven to mediate the cell cycle reentry of cardiomyocytes induced by miR-301a. These findings provide a novel strategy for promoting cardiac repair post-MI.

RESULTS

miRNA Screening Identified miR-301a Overexpressed in the Mammalian Neonatal Cardiomyocytes

During cardiac development and heart morphogenesis in mammals, a high rate of DNA synthesis and cell cycles occurs only in the fetal and neonatal periods, which were associated with cardiomyocyte proliferation and hypertrophic myocardial growth. The cardiomyocyte proliferation rate gradually declines during the late stage of embryogenesis, and it terminates shortly after birth. As such, in contrast with the adult heart, cardiomyocytes in the neonatal heart remain active for rapid growth. In order to identify key genes regulating proliferation and growth of cardiomyocytes, quantitative real-time PCR-based miRNA profiling analyses were performed to compare miRNA expression between the neonatal and adult hearts of mice, and rats as well. Two sets of miRNAs with high expression in neonatal and decrease in the adult hearts were identified from mice (Figure 1A) and rats (Figure 1B). Notably, we found the enrichment of miR-301a in the neonatal cardiomyocytes from both mice and rats, around 20-fold higher in expression compared to adults (Figures 1C and 1D).

In order to confirm the reliability of the miRNA screening results, miR-15b and miR-199a were selected for comparison between our screening data and literature. As mentioned above, these two miRNAs have been reported to promote cardiomyocyte proliferation. Consistent with literature, both miRNAs showed significant higher expression in neonatal cardiomyocytes than that in adult rat (Figure S1), alongside with miR-301a (Figure 1).

In order to determine the cell type highly expressing miR-301a in the heart, cardiomyocytes and fibroblast cells were separated from the neonatal hearts of rats as described previously.[22] Identity and purity of the primary cardiomyocytes were confirmed by immunofluorescence staining of cardiac muscle troponin T (cTnT). As shown in Figures S2A and S2B, the purity of $cTnT^+$ cardiomyocytes reached ~80%. Three cardiomyocyte-specific miRNAs, including miR-1, miR-133a, and miR-499a, were applied to validate the cell type of cardiomyocytes and fibroblasts (Figure S2C). miR-301a showed 3-fold more enrichment in cardiomyocytes than in fibroblast cells (Figure 1E).

miR-301a Promoted Cardiomyocyte Proliferation *In Vitro*

In order to determine the effect of miR-301a on the cell proliferation ability in cardiomyocytes, multiple proliferation assays, including a Cell Counting Kit-8 (CCK-8) assay, a cell cycle analysis, Ki67 staining, 5-ethynyl-2′-deoxyuridine (EdU) staining, and Aurora B staining, were carried out in primary neonatal cardiomyocytes and H9C2 cells as well. As shown in Figures S3A and S3B, overexpression of miR-301a was confirmed in the miR-301a mimic-transfected cells. Increased cell proliferation by enforced expression of miR-301a in H9C2 cells was demonstrated by a CCK-8 assay (Figure 2A). Increased G_1/S transition of the cell cycle by miR-301a overexpression was confirmed using propidium iodide staining and fluorescence-activated cell sorting (FACS) analysis (Figures 2B and 2C). In addition, co-stainings of cardiac marker α-actinin and cell proliferation markers Ki67, EdU and Aurora B were applied to H9C2 cells (Figures 2D and 2E; Figures S4A–S4C) and/or primary neonatal cardiomyocytes (Figures 2F–2I), respectively. The co-stained cells by α-actinin and Ki67 or EdU or Aurora B were considered as proliferating cardiomyocytes. As shown in Figures 2F–2I, both Aurora B and EdU staining on primary neonatal cardiomyocytes demonstrated the induction of the cardiomyocyte proliferation rate from 1.5%–2% to 3.5%–4% by overexpression of miR-301a.

miR-301a Protected Cardiomyocytes against Hypoxia-Induced Cell Apoptosis and Death

Commonly known as a heart attack, MI occurs when a portion of the heart myocardial tissue is damaged after blockage of a coronary artery, causing insufficient oxygen supply. Hypoxia *in vitro* can mimic the situation of MI *in vivo*. In order to determine the effect of miR-301a on cardiomyocytes in response to hypoxia, H9C2 cells were transfected with miR-301a and cultured under the hypoxia condition of 1% oxygen for 24 h, followed by annexin V analysis. The quantities of living cells, early apoptotic cells, late apoptotic cells, and dead cells are shown in Figures 3A and 3B. Quantitative analysis indicated that miR-301a significantly decreased the percentage of apoptotic cells (Figure 3C), while it increased the percentage of surviving cells (Figure 3D) under the hypoxia condition.

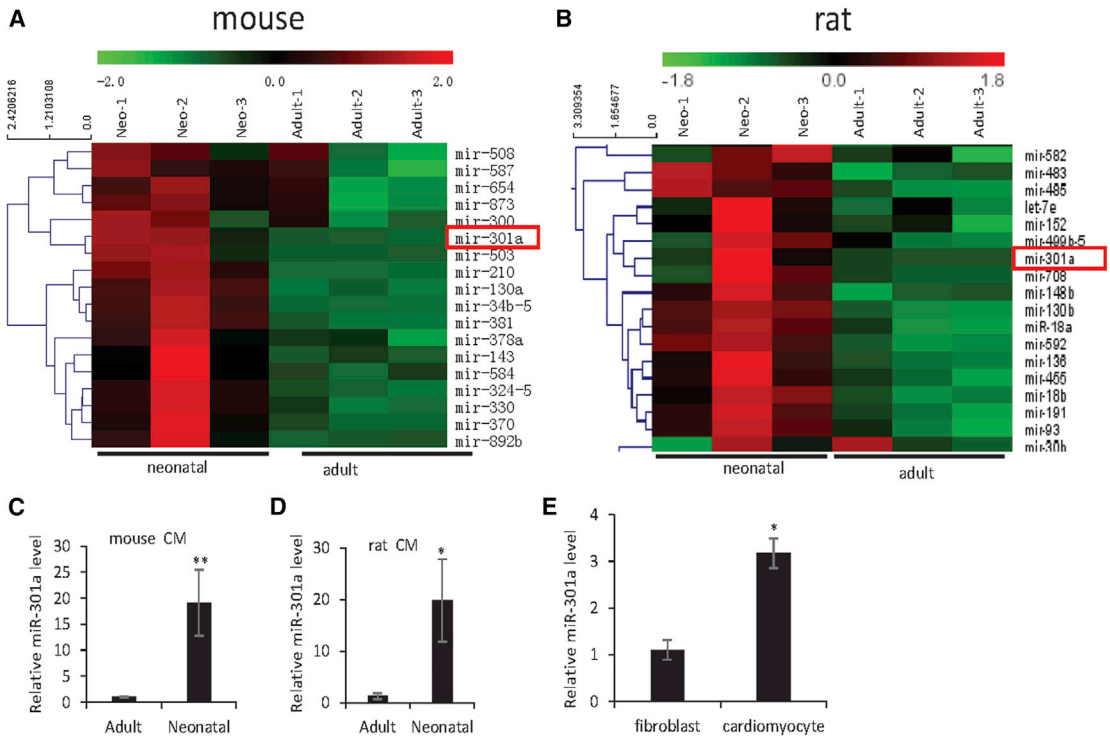

Figure 1. Enrichment of miR-301a in the Mammalian Neonatal Cardiomyocytes

(A) miRNA screening identified a subset of miRNAs with higher expression in the hearts from neonatal mice than adults. (B) miRNA screening identified a subset of miRNAs with higher expression in the hearts from neonatal rats than adults. (C and D) Validation of miR-301a enrichment in the neonatal cardiomyocytes of mice (C) and rats (D) by qRT-PCR analysis. (E) miR-301a showed more enrichment in primary cardiomyocytes compared to cardiac fibroblasts in neonatal rats. Data are mean ± SEM (n = 3). *p < 0.05, **p < 0.01.

AAV9-Mediated miR-301a Delivery of Promoted Post-MI Repair *In Vivo*

In order to determine the effect of miR-301a on post-MI repair *in vivo*, the coronary artery ligation model in mice was applied to mimic human MI. AAV9 virus carrying miR-301a was tail vein-injected to the MI mice at day 3 after surgery for coronary artery ligation. The mice were subsequently monitored for functional recovery of the heart (Figure 4A). In order to confirm the efficiency of cardiac delivery by the AAV9 virus, AAV9-GFP was applied to the control mice following exactly the same protocol as for AAV9-miR-301a administration. In 2 weeks, GFP signals were examined in the heart and liver. Immunofluorescence staining of α-actinin in heart was performed to indicate cardiomyocytes. As shown in Figures 4B and Figure S5, GFP was delivered by the AAV9 system to cardiomyocytes in the heart with an efficiency of about 25%.

For the AAV9-miR-301a-treated MI mice, echocardiography examinations were performed at day 0 before surgery, day 3 before miRNA injection, day 15 after miRNA injection, and day 30 before animal sacrifice (Figures 4A and 4C). All mice survived before sacrifice. The analyses revealed substantial improvement in functional recovery of hearts after AAV9-miR-301a treatment, compared to the control mice (Figures 4C–4I). miR-301a treatment led to significant improvements of the ejection fraction (EF, ~40% in the miR-301a group versus 20% in the negative control [NC] group, Figures 4D–4F), fractional shortening (FS, ~35% in the miR-301a group versus 15% in the NC group, Figure S6A), and left ventricular posterior wall (LVPW) end diastole and end systole (Figure 4G; Figure S6B). Meanwhile, miR-301a treatment partly rescued the change of the left ventricular internal diameter (LVID) end diastole and end systole induced by MI (Figures 4H and 4I).

miR-301a Protected Myocardium and Promoted Myocardium Regeneration *In Vivo*

Additional analyses were performed on the heart of those MI mice treated with AAV9-miR-301a or control. Quantitative analysis of miR-301a indicated an ~2.5-fold increase in expression in the heart of miR-301a group, compared to the control group (Figure S6C). Masson's trichrome staining to the slides demonstrated myocardial fibrosis generated by the coronary artery ligation, while miR-301a treatment protected myocardium from fibrosis as shown in Figures 4J and 4K. In order to examine the size change of cardiomyocytes, cross-sectional areas were analyzed using wheat germ agglutinin (WGA) staining to the heart tissues. As shown in Figures 4L and 4M, MI-induced cardiomyocyte hypertrophy can be partly rescued by the application of miR-301a.

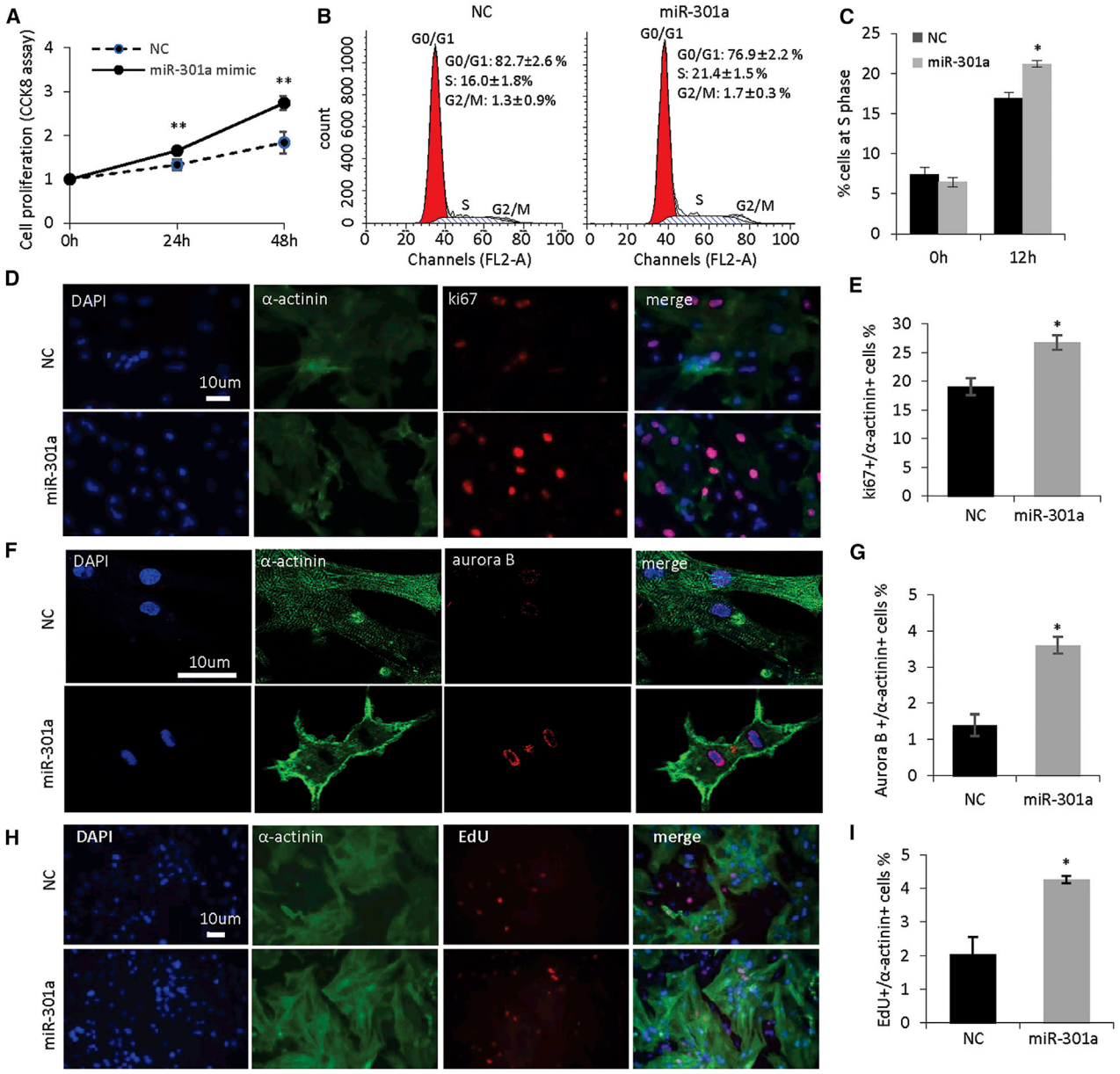

Figure 2. miR-301a Promoted Cardiomyocyte Proliferation

(A) Overexpression of miR-301a promoted cell proliferation in H9C2 cells. (B) The cell cycle analysis indicated an increased G_1/S transition in H9C2 cells by miR-301a overexpression. (C) Quantitative analysis of the cells in the S phase before (0 h) and after (12 h) serum release of the cells with or without overexpression of miR-301a. (D) Ki67 and α-actinin co-staining on H9C2 cells with or without overexpression of miR-301a indicating increased double-positive cell percentage by miR-301a. (E) Quantitative analysis of Figure D. (F) Aurora B and α-actinin co-staining on the primary cardiomyocytes from neonatal rat with or without overexpression of miR-301a indicating increased proliferating cardiomyocytes by miR-301a. (G) Quantitative analysis of Figure F. (H) EdU and α-actinin co-staining on the primary cardiomyocytes further demonstrated the cell proliferation induction by miR-301a. (I) Quantitative analysis of Figure H. Data are mean ± SEM (n = 3). *p < 0.05, **p < 0.01.

To determine the effect of miR-301a on cell proliferation of adult cardiomyocytes *in vivo*, co-staining for α-actinin and Ki67 was applied to the slides from the paraffin-embedded heart tissues. As seen in Figures 4N and 4O and Figure S6D, ~1.5%–2.0% of adult cardiomyocytes in the miR-301a-treated mice were double positive to α-actinin and Ki67, compared to ~0.5%–1.0% in the control mice, indicating the improved proliferative ability of cardiomyocytes by miR-301a *in vivo*.

In view of the cardiac cellular protection against hypoxia stimulation by miR-301a *in vitro* (Figure 3), several apoptotic factors were examined in the heart of MI mice with or without treatment by miR-301a,

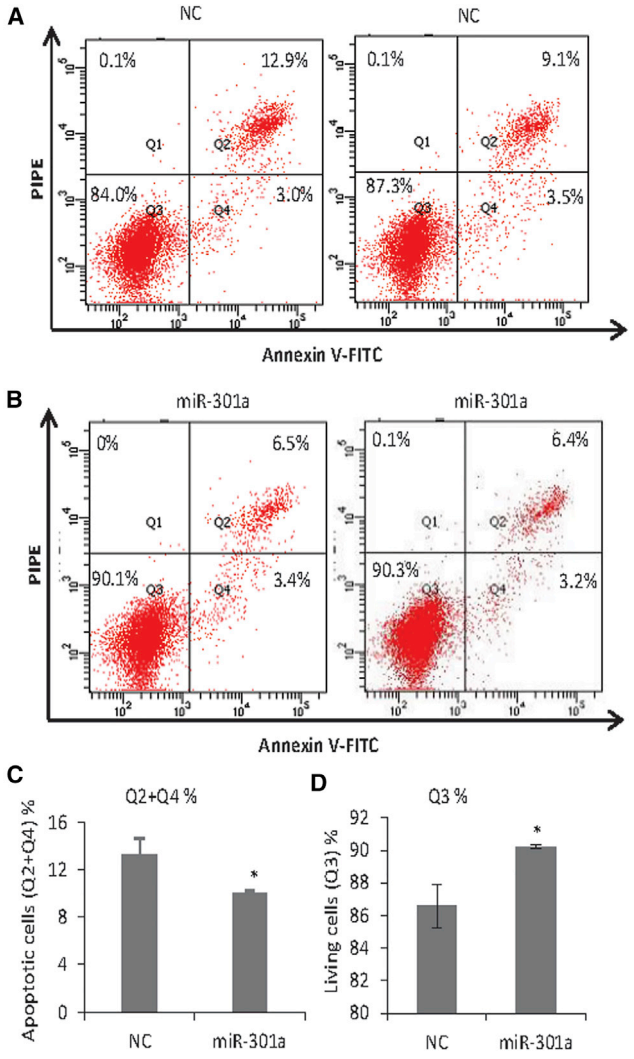

Figure 3. miR-301a Protected Cardiomyocytes against Hypoxia-Induced Cell Apoptosis

(A and B) H9C2 cells were transfected with RNA oligonucleotide negative control (NC) (A) or miR-301a mimic (B) and cultured under the hypoxia condition with 1% oxygen for 24 h followed by annexin V analysis. The percentages of living cells, early apoptotic cells, late apoptotic cells, and dead cells are indicated. (C) Quantitative analysis indicated fewer apoptotic cells in the miR-301a group compared to the NC. (D) Quantitative analysis indicated more survived cells in the miR-301a group compared to the NC. Data are mean ± SEM (n = 3). *$p < 0.05$.

determining the cardiac protection by miR-301a *in vivo*. As shown in Figure S7, upregulation of anti-apoptotic factor Bcl2 and downregulation of apoptotic factor Bax after miR-301a treatment were detected in the heart.

PTEN Is a Target Gene of miR-301a in Cardiomyocytes

In order to determine the mechanism by which miR-301a protects myocardium and regulates myocardial regeneration, a bioinformatics analysis using miRNA target prediction tools, including TargetScan and miRanda, identified 2,209 predicted target genes of miR-301a in rats and 2,345 in mice. Meanwhile, 487 heart development-related genes were identified from a public database. 21 genes were overlapped among the three sets of the identified genes (Figures 5A and 5B). Further validation assays by quantitative RT-PCR analyses demonstrated 4 of the 21 genes showing downregulation in cardiomyocytes by miR-301a, including PTEN, SMAD4, TIMP2, and TGFBR2 (Figure 5C). In consideration of the function of PTEN in regulating cell survival and proliferation, the interactions between miR-301a, PTEN, and cardiac cell proliferation were further determined. As shown in Figure 5D, three binding sites to miR-301a were identified from the 3′ UTR of rat PTEN mRNA. Luciferase reporter vectors carrying either wild-type (WT) or point-mutated (MU) PTEN 3′ UTR were assayed, demonstrating the direct interaction between PTEN 3′ UTR and miR-301a (Figure 5E). The inhibition of PTEN at the protein level by miR-301a *in vivo* was validated in the hearts from AAV9-miR-301a-treated mice (Figure 6). Notably, our recent work also demonstrated downregulation of PTEN by miR-301a in the mouse ESC-differentiated cardiomyocytes[27].

PTEN/PI3K/AKT Mediated miR-301a Regulation of Cardiac Cell Proliferation

In order to determine the function of PTEN in miR-301a-regulated cell proliferation in cardiomyocytes, PTEN small interfering RNA (siRNA) was applied to H9C2 cells followed by EdU staining to determine the change of cell proliferation rate. miR-301a transfection was applied for comparison. Among the three siRNA candidates, si-1 and si-3 showed ~70% knockdown of PTEN (Figure S8). As such, a mixture of si-1 with si-3 (1:1) was used for experiments thereafter. As seen in Figures 6A and 6B, PTEN knockdown can mimic the miR-301a overexpression in cardiomyocytes, promoting cell proliferation from ~10% to ~25%. Moreover, reintroduction of PTEN back-attenuated the cell proliferative induction by miR-301a in H9C2 cells (Figures 6C and 6D), demonstrating that PTEN mediates the miR-301a function in promoting cell proliferation in cardiomyocytes.

It has been well confirmed that PTEN is frequently mutated in tumors and functions as a tumor suppressor arresting the cell cycle at the G_1 phase mostly through the phosphatidylinositol 3-kinase (PI3K)/AKT pathway. The PTEN/PI3K/AKT signaling pathway is involved not only in tumorigenesis, but also in a wide variety of heart diseases, including myocardial hypertrophy, heart failure, and preconditioning.[28,29] In order to determine whether the PI3K/AKT pathway is involved in the miR-301a-PTEN regulation of cardiomyocyte proliferation, proteomic analysis was applied to the miR-301a-treated mouse heart, as well as H9C2 cells. As shown in Figure 6E, downregulation of PTEN was accompanied with upregulation of phosphorylated (p-)AKT and p-GSK-3β in the heart tissues of miR-301a-treated mice. Similar results were confirmed in the miR-301a overexpressed H9C2 cells, leading to increased expression of cyclin D1 (Figures S9A and S9B). These *in vitro* and *in vivo* data strongly suggest the involvement of PTEN/PI3K/AKT signaling in mediation of miR-301a-induced cell proliferation in cardiomyocytes.

In order to further determine the mechanism through which PI3K/AKT mediates miR-301a-induced cardiomyocyte proliferation, a

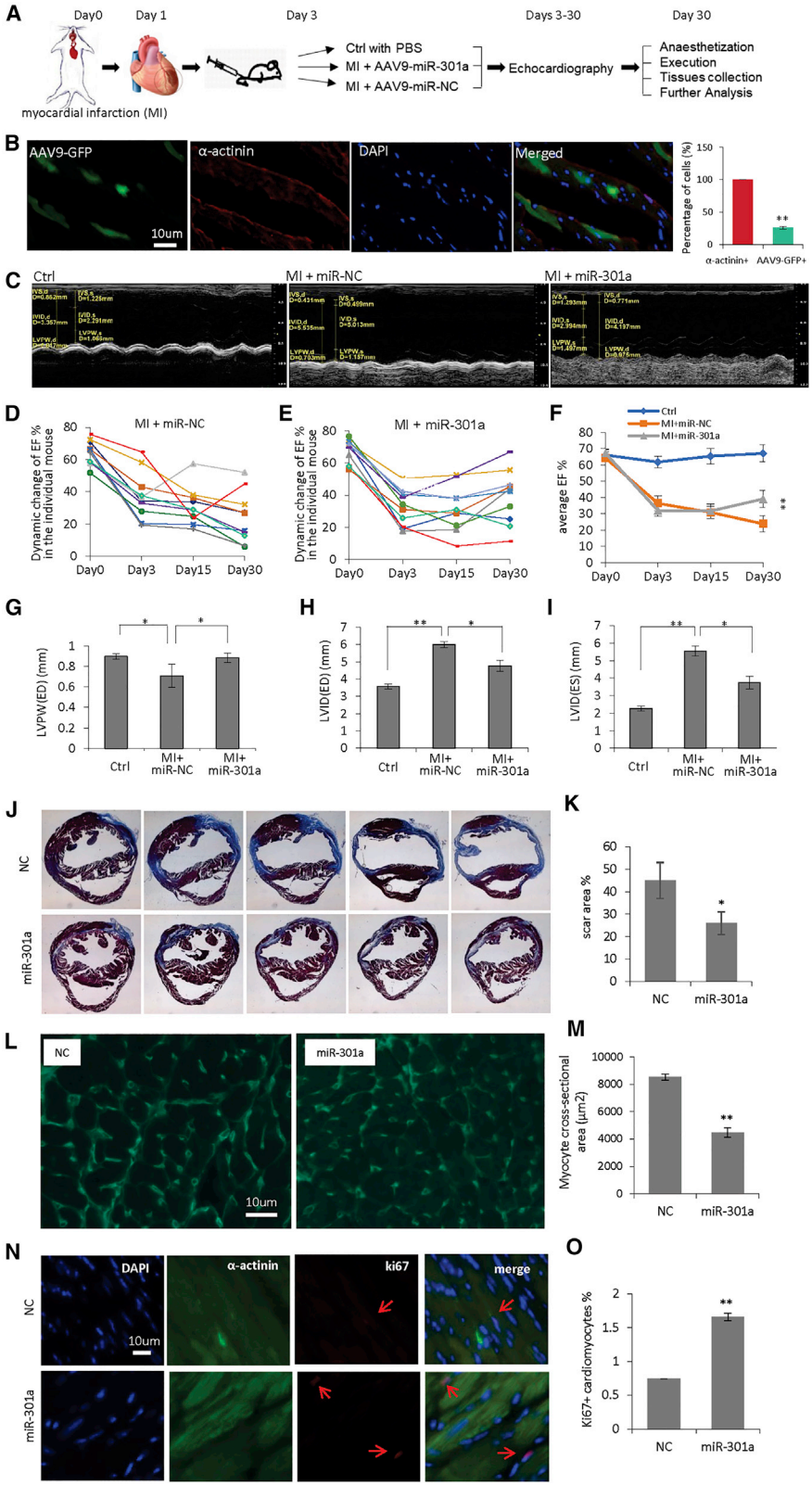

(legend on next page)

highly selective small molecule inhibitor of AKT, RG7440, was applied to H9C2 cells. RG7440 binds to and blocks the activation of AKT, resulting in cell cycle arrest and cell proliferation suppression. RG7440 induced an increase in AKT phosphorylation. Despite this increase in p-AKT, downstream AKT signaling activity was inhibited.[30] Herein, an increase of p-AKT, a decrease of p-GSK-3β, and a decrease of cyclin D1 were detected in H9C2 cells after treatment with 5 nM RG7440 (Figure 6F). Moreover, RG7440 treatment not only suppressed cell proliferation via inhibiting endogenous AKT activity (Figure 6G, control [Ctrl] groups), but it also blocked miR-301a-induced cell proliferation (Figure 6G, miR-301a groups), further demonstrating that AKT signaling mediated miR-301a-induced cell proliferation in cardiomyocytes.

DISCUSSION

Cardiovascular diseases, including heart failure, heart arrhythmia, cardiogenic shock, cardiac arrest, and others, are becoming the leading cause of death all over the world. They remain incurable due to the limited ability to replace damaged or lost cardiomyocytes after injury in the heart. Activation of endogenous cardiomyocyte renewal may provide a new approach for cardiac repair after injury. In mammals shortly after birth, a transition from hyperplastic to hypertrophic myocardial growth is associated with ceased DNA synthesis and an exited cell cycle in cardiomyocytes.[31,32] Although the vast majority of adult cardiomyocytes grow predominantly in cell size, not in cell number, emerging evidence has demonstrated that adult cardiomyocytes can reenter the cell cycle and produce new cardiomyocytes after ischemic injury.[2,3,33] However, the mechanisms regulating cardiogenesis remain to be understood. Approaches for induction of the cell cycle reentry and regeneration of new cardiomyocytes remain to be developed.

As reviewed previously,[34,35] different approaches have been applied to regenerate new cardiomyocytes, including induction of the cell cycle reentry, activation of endogenous cardiac stem cells or progenitor cells, and stimulation of endogenous heart regeneration through reprogramming cardiac fibroblasts into cardiomyocytes. Emerging evidence has demonstrated that non-coding miRNAs are capable of maintaining cardiac organ homeostasis and repairing injured heart in adult mammals.[6,24–26] A recent publication reported miR-128 serving as a critical regulator of endogenous cardiomyocyte proliferation.[36] Deletion of miR-128 promoted cell cycle re-entry in adult cardiomyocytes, and thereby reduced the levels of fibrosis and attenuated cardiac dysfunction in response to MI.[36] The miR-17-92 cluster, as a critical regulator of cardiomyocyte proliferation, is required and sufficient to induce cardiomyocyte proliferation in the postnatal and adult hearts.[25] The miR-302–367 cluster encouraged embryonic cardiomyocyte proliferation. The infarcted mouse hearts treated with the miR-302–367 cluster exhibited decreased cardiac fibrosis and improved heart function.[37] A miRNA prosurvival cocktail including miR-21, miR-24, and miR-221 was demonstrated to improve the engraftment of transplanted cardiac progenitor cells and therapeutic efficacy for treatment of ischemic heart disease.[38] Our current study demonstrated that overexpression of miR-301a is able to induce cardiomyocytes proliferation. Cardiac delivery of miR-301a promoted regeneration of damaged heart *in vivo*. In addition, miR-301a protects cardiomyocytes against hypoxia-induced apoptosis.

In view of the importance of endocardium and cardiac endothelial cells in regulating cardiomyocyte proliferation and myocardium regeneration, we are curious whether miR-301a has expression and regulating function in cardiac endothelial cells. McCall et al.[39] screened miRNA profiling of diverse endothelial cell types including human aorta endothelial cells (HAECs), human coronary artery endothelial cells (HCECs), human umbilical vein endothelial cells (HUVECs), as well as epithelial cells and hematologic cells. They found that miR-301a is expressed only in epithelial cells and hematologic cells, but not endothelial cells, which is consistent with our finding that heart delivery of miR-301a *in vivo* promoted cardiac repair post-MI through regulating cell proliferation and/or survival in cardiomyocytes.

It has to be taken into account that emerging evidence indicated the oncogenic function of miR-301a in regulating cancer-related differentiation, apoptosis, and pathogenesis in multiple tumor types.[40] High expression of miR-301a has been reported in gastric cancer,[41] pancreatic cancer,[42] hepatocellular cancer,[43] and colorectal cancer,[44] which

Figure 4. AAV9-Mediated miR-301a Delivery Promoted Post-MI Repair *In Vivo*

(A) Schematic representation of the procedure for tail vein injection of AAV9-miR-301a to the MI model of mice, followed by echocardiography monitoring. (B) AAV9-GFP was applied to the mice by tail vein injection following the exact same protocol as for AAV9-miR-301a administration. GFP signaling and α-actinin staining on the heart tissue in 2 weeks indicating the GFP delivery to cardiomyocytes *in vivo*. The α-actinin$^+$ cells and GFP$^+$/α-actinin$^+$ cells were counted under a microscope to quantify the delivery efficiency. Data are mean ± SEM (n = 3). $^{**}p < 0.01$. (C) Representative echocardiography images of normal control mice, as well as MI mice treated with miR-301a or NC. (D) The ejection fraction change of the individual mice in the control group (n = 10) from day 0 before surgery, day 3 before miRNA injection, day 15 after miRNA injection, and day 30 before animal sacrifice. (E) The ejection fraction change of the individual mice in miR-301a group (n = 10). (F) The average ejection fraction values at the above time points of the mice in the PBS control group, the miR-301a-treated MI group, and the NC-treated MI group. (G) Left ventricular posterior wall (LVPW) end diastole of the mice in the PBS control group, the miR-301a-treated MI group, and the NC-treated MI group. (H and I) Left ventricular internal diameter (LVID) end diastole (H) and end systole (I) of the mice in the PBS control group, the miR-301a-treated MI group, and the NC-treated MI group. (J) Masson's trichrome staining to the heart slides from the apex to the left anterior descending (LAD) artery sites demonstrating that mir-301a treatment protected myocardium from scar fibrosis generated by the coronary artery ligation. (K) Quantitative analysis of (J). (L) Cross-sectional areas analysis by WGA staining to the heart slides demonstrating that miR-301a treatment protected cardiomyocytes against MI-induced hypertrophy. (M) Quantitative analysis of (L). (N) Ki67 and α-actinin co-staining on the slides from paraffin-embedded MI heart tissue demonstrating more double-positive cardiomyocytes in the AAV9-miR-301a group. Representative proliferating cardiomyocytes are indicated with red arrows. (O) Quantitative analysis of (N). Data are mean ± SEM (n = 10). $^{*}p < 0.05$, $^{**}p < 0.01$.

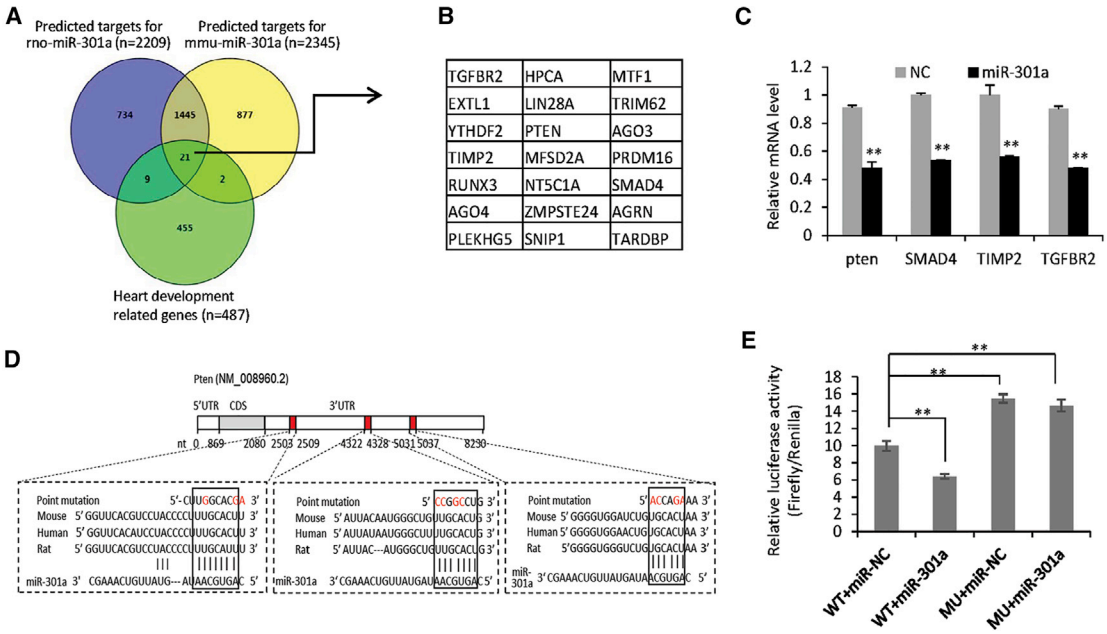

Figure 5. PTEN is a Target Gene of miR-301a in Cardiomyocytes

(A) Comparison between 2,209 predicted target genes of miR-301a in rats, 2,345 predicted target genes of miR-301a in mice, and 487 genes related to heart development. (B) The list of 21 genes overlapped in Figure A. (C) qRT-PCR analysis validated downregulation of PTEN, SMAD4, TIMP2, and TGFBR2 expression by miR-301a in cardiomyocytes. (D) Sequence BLASTN analysis identified three binding sites to miR-301a at the 3′ UTR region of PTEN mRNA. The three binding sites are highly conserved between humans, mice, and rats. Luciferase reporter vectors carrying either wild-type (WT) or point-mutated (MU, mutated nucleotides are indicated with red font) PTEN 3′ UTR were cloned. (E) Luciferase reporter assays demonstrated the increased luciferase activity in the MU vector compared to the WT. Co-transfection of miR-301a inhibited luciferase activity in the WT, but not MU, vector. Data are mean ± SEM (n = 3). *$p < 0.05$, **$p < 0.01$.

correlated with the invasion and migration of the disease. As such, the risk assessment of tumorigenesis is fully required before clinical application of miR-301a in treatment of patients with heart injury. Development of novel materials or methods for local delivery to the heart or cardiomyocyte-specific overexpression of miR-301a will be a solution to avoid the tumorigenic side effect. In particular, seeing that heart is the organ that rarely grows primary tumors, the cardiomyocyte-targeted delivery of miR-301a is a relatively safe and applicable approach.

Herein, the tumor suppressor gene PTEN is identified as a direct target of miR-301a in regulating cardiomyocyte proliferation. It has been well confirmed that PTEN plays essential roles in the control of tumorigenesis.[45,46] The focal adhesion kinase (FAK) pathway, the mitogen-activated protein kinase (MAPK) pathway, and the PI3K/AKT pathway have been demonstrated to be downstream signaling of PTEN.[47–49] Mostly PTEN dephosphorylates PIP3 (phosphatidylinositol (3,4,5)-trisphosphate) to PIP2 (phosphatidylinositol (4,5)-bisphosphate), thereby arresting the cell cycle at the G_1 phase through the PI3K/AKT pathway,[49] which has been reported to be involved in a wide variety of cardiovascular diseases, regulating survival, proliferation, apoptosis, hypertrophy, and contractility of cardiac cells.[50] In the current study, PTEN was identified as a target gene of miR-301a in cardiomyocytes. Suppression of PTEN was responsible for activating PI3K/AKT signaling by miR-301a, thereby promoting cell proliferation in cardiomyocytes (Figure 6H). Cyclin D1, as a key gene downstream of PI3K/AKT, showed significant upregulation by miR-301a in cardiomyocytes. Application of RG7440 (a small molecule inhibitor of AKT) to cardiomyocytes not only resulted in the inactivation of AKT signaling, but it also reversed the miR-301a-induced cell proliferation. As such, the PTEN/PI3K/AKT pathway functions as a bridge to connect miR-301a to cyclin D1 expression and cell proliferation in cardiomyocytes, clearly demonstrating a potential mechanism for regulating the cell cycle reentry of cardiomyocytes.

Oxidative stress and apoptosis play fundamental roles in myocardial injury.[51] Many heart diseases, including MI, occur due to the blockage of a coronary artery and insufficient oxygen supply. Although the literature has suggested that silencing PTEN alone can lead to reduced apoptosis and improved cell survival in H_2O_2-treated H9C2 cardiomyocytes,[52] whether the cardiomyocyte protection from hypoxia by miR-301a was mediated by PTEN or other target genes is yet to be determined.

In summary, our findings provide a novel candidate of miRNA, miR-301a, for induction of the cell cycle reentry and protection of hypoxic injury in adult cardiomyocytes. Moreover, it suggests a novel strategy (such as PTEN siRNA or AKT activator) targeting PTEN/PI3K/AKT signaling to improve cardiac repair after injury.

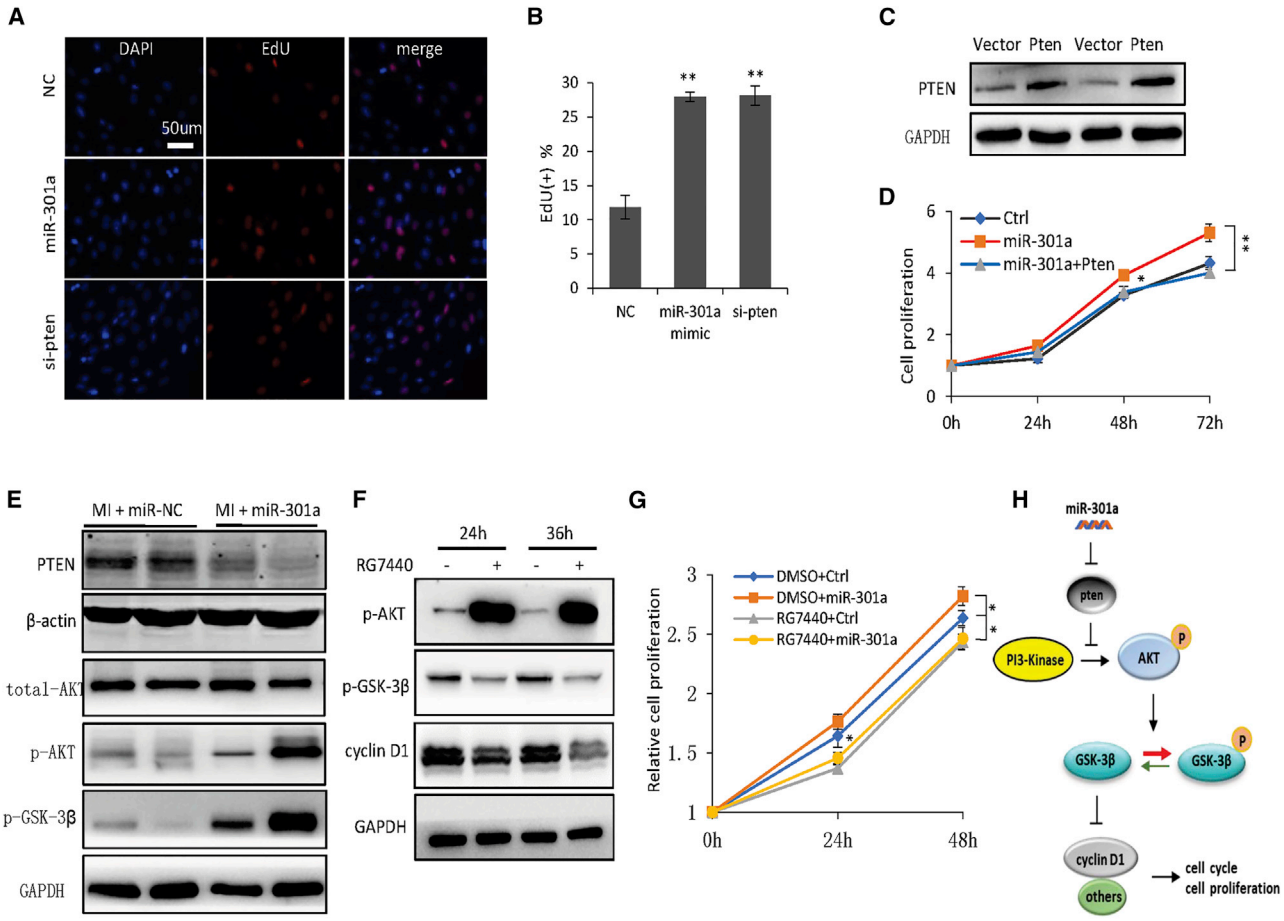

Figure 6. PTEN/PI3K/AKT Signaling Mediated miR-301a Regulation of Cell Proliferation in Cardiomyocytes

(A) miR-301a mimic, PTEN siRNA, and an NC were applied to H9C2 cells, respectively, followed by EdU staining, indicating that both PTEN knockdown and miR-301a overexpression promoted cardiomyocyte proliferation. (B) Quantitative analysis of (A). (C) Western blot analysis demonstrating the upregulation of PTEN at the protein level in H9C2 cells after transfection with PTEN plasmid. (D) Introduction of PTEN back into the miR-301a-treated H9C2 cells attenuated the cell proliferative induction by miR-301a. (E) Western blot analyses demonstrating that upregulation of p-AKT and p-GSK-3β were associated with downregulation of PTEN in the hearts from AAV9-miR-301a-treated mice. (F) Western blot analyses demonstrating increased p-AKT and decreased p-GSK-3β and cyclin D1 in H9C2 cells by application of RG7440, a small molecule inhibitor of AKT. (G) CCK-8 assays demonstrating that RG7440 treatment in H9C2 cells not only suppressed cell proliferation via inhibiting endogenous AKT activity (Ctrl groups), but also reversed the miR-301a-induced cell proliferation (miR-301a groups). (H) Cartoon representation of mechanisms for the PTEN/PI3K/AKT signaling pathway mediating the miR-301a regulation of cardiac cell proliferation. Data are mean ± SEM (n = 3). *p < 0.05, **p < 0.01.

MATERIALS AND METHODS

Animals

Animal studies were approved by the Institutional Animal Care and Use Committee of the Tongji University Shanghai East Hospital for Laboratory Animal Medicine. SD rats and C57BL/6J male mice were purchased from Silaike Animal Company (Shanghai, China). Before treatment, all animals were screened for the baseline determination of echocardiography using the Vevo 2100 imaging system (VisualSonics, Canada). Cardiac injury was generated by coronary artery ligation using silk sutures or sham surgery to 8-week-old adult mice. Echocardiography was performed for each cardiac injured mouse at day 3 after surgery, followed by tail vein injection with AAV9-miR-301a or AAV9-miR-scramble (100 μL containing ~5 × 10^{11} vector genomes [vg] per mouse). Sham surgery mice given the same volume of 1× PBS were used as the normal control group.

Cells

Cell line H9C2 was purchased from ATCC and maintained in Dulbecco's modified Eagle's medium (DMEM) with 10% of fetal bovine serum (FBS), penicillin (100 U/mL), and streptomycin (100 μg/mL).

The neonatal rat ventricular myocytes (NRVMs) were isolated and cultured as described previously.[22] Briefly, heart tissues from 2-day-old neonatal rats were cut into pieces and digested with 1× PBS containing 0.1% collagenase II and 0.002% DNase to a single-cell suspension, and cultured in DMEM containing 10% FBS, penicillin

(100 U/mL), and streptomycin (100 μg/mL). 10 μM 5-bromo-2′-deoxyuridine (BrdU) (Sigma) was applied to the medium to reduce fibroblast content. Additional cardiofibroblasts were removed from cardiomyocytes using differential adhesion. Purified cardiomyocytes were seeded on 0.1% gelatin-coated plates. After 48 h of cultivation, the NRVMs were transfected with indicated miRNA for further analysis.

miRNA, siRNA, Plasmid, and Transfection

miR-301a mimic and scrambled NC oligonucleotides were synthesized by GenScript (Nanjing, China). The miRNA mimic sequence for the miR-301a sense strand is 5′-r(CAGUGCAAUAGUAUUGUCAAAGC)dTdT-3′. A scrambled RNA sequence was used for miRNA NC: 5′-r(UGGGCGUAUAGACGUGUUACAC)dTdT-3′. PTEN siRNAs (target sequence 5′-GGGAAAGGACGGACUGGUG-3′, 5′-AAAGGUGAAGAUCUACUCC-3′, 5′- GAGUAACUAUUCCCAGUCA-3′) were synthesized by Genomeditech (Shanghai, China). The target sequence for NC siRNA is 5′-AGTCGCATACCTCGACAATAAT-3′. PCDNA3.1 was used to clone PTEN-expressing plasmid. Cell transfection was performed using Lipofectamine RNAiMAX from Invitrogen (for small RNA) or HiPerFect reagent from QIAGEN (for plasmid) following the manufacturer's instructions. A final concentration of 50 nM miRNA mimic or siRNA was used for *in vitro* assays.

Immunofluorescence

Cells were fixed with 4% paraformaldehyde for 15 min and permeabilized with 0.5% Triton X-100 (Sigma) in 1× PBS for 10 min at room temperature. After 1× PBS washing, 4% FBS was used for blocking for 1 h at room temperature. Then, cells were incubated with the primary antibodies (1:10 to 1:100 dilution), including anti-α-actinin (Sigma, A7811), anti-Ki67 (Abcam, ab15580), anti-Aurora B (Abcam, ab2254) or anti-cTnT (sc-20025, Santa Cruz) overnight at 4°C, and the secondary antibody conjugated to Alexa Fluor 488 (Invitrogen, A11001) or Alexa Fluor 555 (Invitrogen, A21428) for 1 h at room temperature. The nucleus was stained with 4′,6-diamidino-2-phenylindole (DAPI, Sigma, D9542) for 30 min at room temperature. For EdU staining, the culture medium containing 10 μM EdU (Invitrogen, C10339) was applied to H9C2 or NRVM cells for 2 or 24 h, respectively, followed by EdU analysis using Click-iT EdU imaging kits (Invitrogen). All slides were imaged using fluorescence microscopy (Leica, Germany).

Cell Apoptosis Assay

Cells were cultured under hypoxia condition (1% O_2, 94% N_2, 5% CO_2) for 24 h, followed by annexin V-FITC/immunoprecipitation (IP) kit (Bestbio, China) according to the manufacturer's instructions, and analyzed with flow cytometry (BD FACSAria II).

Cell Proliferation Assays

1×10^4 cells/well were seeded into 96-well plates. After culturing for 24–72 h as indicated, the cells were stained with 10 μL/well CCK-8 solution for 2 h at cell-culturing condition, then determining the cell growth by measuring the absorbance at 450 nm.

Cell Cycle Analysis

Medium containing 0.5% FBS was used for cell starvation for 24 h, followed by regular medium with 10% FBS to induce the cell cycle. Cells were processed by standard methods using propidium iodide staining of DNA. 10,000 cells per sample were analyzed by flow cytometry with a FACScan flow cytometer (BD Biosciences, Mansfield, MA, USA). Since the DNA content in cells varies upon the cell cycle stages, the cells that are in G_0/G_1, S, or G_2 phases were calculated separately according to the signal of propidium iodide DNA-binding dyes.

Masson's Trichrome Staining

Slides from paraffin-embedded heart tissues were stained for fibrosis analysis using a Masson's trichrome staining kit (BA4079B, Baso, China). The fibrotic areas were stained with blue, and the normal areas were stained with red. The percentage of scar size was estimated from fibrotic area over total left ventricular area using a M205 stereomicroscope (Leica, Germany) and analyzed with Image-Pro Plus 6.0 software.

WGA Staining

Slides from paraffin-embedded heart tissues were stained with FITC-conjugated anti-WGA (Sigma). The mean cross-sectional area was calculated from ∼150 cardiomyocytes with a nucleus in three randomly selected fields per group. Images were captured by fluorescence microscopy (Leica, Germany) and analyzed with Image-Pro Plus 6.0 software.

miRNA qRT-PCR Analysis

An M&G miRNA reverse transcription kit (miRGenes, Shanghai, China) was used to prepare the first-strand cDNA of miRNAs following the manufacturer's instruction. 100 ng of purified total RNA from each sample was used for miRNA measurement. After reverse transcription, the cDNA was diluted 1:1,000 for real-time PCR. Forward primer sequences for real-time PCR of miRNAs were as follows: miR-301a, 5′-CCAGTGCAATAGTATTG-3′; miR-1, 5′-CCTGGAATGTAAAGAAGTATG-3′; miR-133a, 5′-TTGGTCCCCTTCAACCAGCTG-3′; miR-499a, 5′-GACUUGCAGUGAUGUUU-3′; miR-15b, 5′-TAGCAGCACATCATGGTT-3′; miR-17-5p, 5′-CAAAGTGCTTACAGTGC-3′; miR-18a, 5′-GGTGCATCTAGTGCAGATAG-3′; miR-18b, 5′-GGTGCATCTAGTGCAGTTAG-3′; miR-19a, 5′-CCTGTGCAAATCTATGCAA-3′; miR-92a, 5′-ATTGCACTTGTCCCGGCCTG-3′; miR-199a, 5′-CAGTGTTCAGACTACCTGT-3′; 5S rRNA, 5′-AGTACTTGGATGGGAGACCG-3′. A universal reverse primer was provided by miRGenes. SYBR Green master mix was purchased from Applied Biosystems/Life Technologies. The ABI Q6 sequence detection system (Applied Biosystems/Life Technologies) was used to run quantitative real-time PCR. 5S rRNA was used for normalization.

miRNA Profiling Analysis in the Heart of Neonatal and Adult Rodents

Total RNA was isolated from plasma specimens with TRIzol reagent (Life Technologies). The cDNA was prepared as described above. The miRNA profiling analyses were performed with the quantitative

real-time PCR-based miRNA panel that contains 365 mammalian cell-enriched miRNAs and reference small RNA 5S rRNA (miRGenes, Shanghai, China). 5S rRNA was used for normalization to calculate ΔCt. Neonatal and adult were compared to calculate ΔΔCt and fold change. MeV (version 4.9) software was used for further data analysis. $p < 0.05$ was considered as significant.

Western Blot Analysis

Cell lysates (50 μg) prepared with radioimmunoprecipitation assay (RIPA) buffer containing protease inhibitor cocktail (Roche Diagnostics) were separated by 10% SDS-PAGE. The proteins were transferred to polyvinylidene fluoride (PVDF) membranes. 5% non-fat milk (w/v) was used for the blocking step. The following primary antibodies (1:2,000) were used: PTEN (sc-7974, Santa Cruz), total AKT (4691, Cell Signaling Technology), p-AKT (4060T, Cell Signaling Technology), p-GSK-3β (5558T, Cell Signaling Technology), cyclin D1 (sc-20041, Santa Cruz), Bcl-2 (sc-492, Santa Cruz), Bax (2772S, Cell Signaling Technology), and β-actin (sc-47778, Santa Cruz). GAPDH (5174, Cell Signaling Technology), horseradish peroxidase (HRP)-linked anti-rabbit immunoglobulin G (IgG) (7074S, Cell Signaling Technology), and HRP-linked anti-mouse IgG (7076S, Cell Signaling Technology) were used as secondary antibodies (1:3,000).

Gene Reporter Assays

The WT PTEN 3′ UTR luciferase reporter and points mutation to the miR-301a binding sites were generated with pMIR-REPORT Luciferase vector. For cellular transfection with reporter DNA, actively growing cells were seeded on 12-well plates at a density of 5×10^4 cells/well. The next day, cells were co-transfected using Lipofectamine 2000 (Invitrogen) with 1.0 μg of PTEN 3′ UTR luciferase reporter and 0.2 μg of Renilla luciferase. Twenty-four hours after transfection, luciferase activities were measured using the Dual-Luciferase reporter assay system (Promega, Madison, WI, USA) by AutoLumat.

AAV9 Virus Preparation and *In Vivo* Assays

Mouse precursor (pre-)miR-301a or control sequences were cloned into the vector GPAAV-CMV-MCS-WPRE, followed by infection to prepare AAV9. The preparation and purification of the AAV were performed by the Genomeditech (Shanghai, China). AAV9-miR-301a or AAV9-miR-scramble viruses were tail vein injected into the MI model mice with $\sim 5 \times 10^{11}$ vg per mouse in 100 μL of PBS. As a control, similarly constructed and prepared AAV9-GFP virus was tail vein injected into control mice to track the GFP signaling in the heart and other tissues.

Statistical Analysis

Data are presented as mean ± SEM. The standard two-tailed Student's t test was used for statistical analysis, in which $p < 0.05$ was considered significant.

SUPPLEMENTAL INFORMATION

Supplemental Information can be found online at https://doi.org/10.1016/j.omtn.2020.08.033.

AUTHOR CONTRIBUTIONS

L.Z. performed the cellular and molecular assays *in vivo* and *in vitro*. Q.Z. and S.D. carried out miRNA screening and molecular assays. Q.Z., L.Z., and H.F. participated in the statistical analysis. L.Z., J.L., and Z.X. contributed to western blot and gene reporter assays. L.Z., Q.Z., and Y.Z. organized figures and supplemental information. L.Z. and Q.Z. revised the partial manuscript. Z.Y., X.C., Z.L., and Y.G. designed research and wrote the manuscript.

CONFLICTS OF INTEREST

The authors declare no competing interests.

ACKNOWLEDGMENTS

This work was supported by Grant 81800243 from the National Natural Science Foundation of China, Grant 18411965900 from the Science and Technology Commission of Shanghai Municipality, and by Grants 22120180103 and 22120180125 from the Fundamental Research Funds for the Central Universities.

REFERENCES

1. Rubart, M., and Field, L.J. (2006). Cardiac regeneration: repopulating the heart. Annu. Rev. Physiol. *68*, 29–49.
2. Deng, S., Zhao, Q., Zhen, L., Zhang, C., Liu, C., Wang, G., Zhang, L., Bao, L., Lu, Y., Meng, L., et al. (2017). Neonatal heart-enriched miR-708 promotes proliferation and stress resistance of cardiomyocytes in rodents. Theranostics *7*, 1953–1965.
3. Wang, W.E., Li, L., Xia, X., Fu, W., Liao, Q., Lan, C., Yang, D., Chen, H., Yue, R., Zeng, C., et al. (2017). Dedifferentiation, proliferation, and redifferentiation of adult mammalian cardiomyocytes after ischemic injury. Circulation *136*, 834–848.
4. Priori, S.G., Napolitano, C., Di Pasquale, E., and Condorelli, G. (2013). Induced pluripotent stem cell-derived cardiomyocytes in studies of inherited arrhythmias. J. Clin. Invest. *123*, 84–91.
5. Kajstura, J., Urbanek, K., Perl, S., Hosoda, T., Zheng, H., Ogórek, B., Ferreira-Martins, J., Goichberg, P., Rondon-Clavo, C., Sanada, F., et al. (2019). Retraction. Circ. Res. *124*, e22.
6. Eulalio, A., Mano, M., Dal Ferro, M., Zentilin, L., Sinagra, G., Zacchigna, S., and Giacca, M. (2012). Functional screening identifies miRNAs inducing cardiac regeneration. Nature *492*, 376–381.
7. Yutzey, K.E. (2017). Cardiomyocyte proliferation: teaching an old dogma new tricks. Circ. Res. *120*, 627–629.
8. De Falco, M., Cobellis, G., and De Luca, A. (2009). Proliferation of cardiomyocytes: a question unresolved. Front. Biosci. (Elite Ed.) *1*, 528–536.
9. Zebrowski, D.C., and Engel, F.B. (2013). The cardiomyocyte cell cycle in hypertrophy, tissue homeostasis, and regeneration. Rev. Physiol. Biochem. Pharmacol. *165*, 67–96.
10. Beltrami, A.P., Barlucchi, L., Torella, D., Baker, M., Limana, F., Chimenti, S., Kasahara, H., Rota, M., Musso, E., Urbanek, K., et al. (2003). Adult cardiac stem cells are multipotent and support myocardial regeneration. Cell *114*, 763–776.
11. Kubin, T., Pöling, J., Kostin, S., Gajawada, P., Hein, S., Rees, W., Wietelmann, A., Tanaka, M., Lörchner, H., Schimanski, S., et al. (2011). Oncostatin M is a major mediator of cardiomyocyte dedifferentiation and remodeling. Cell Stem Cell *9*, 420–432.
12. Turan, R.D., Aslan, G.S., Yücel, D., Döğer, R., and Kocabaş, F. (2016). Evolving approaches to heart regeneration by therapeutic stimulation of resident cardiomyocyte cell cycle. Anatol. J. Cardiol. *16*, 881–886.
13. Bersell, K., Arab, S., Haring, B., and Kühn, B. (2009). Neuregulin1/ErbB4 signaling induces cardiomyocyte proliferation and repair of heart injury. Cell *138*, 257–270.
14. Bartel, D.P. (2004). MicroRNAs: genomics, biogenesis, mechanism, and function. Cell *116*, 281–297.

15. Li, Y., Liang, C., Ma, H., Zhao, Q., Lu, Y., Xiang, Z., Li, L., Qin, J., Chen, Y., Cho, W.C., et al. (2014). miR-221/222 promotes S-phase entry and cellular migration in control of basal-like breast cancer. Molecules *19*, 7122–7137.

16. Cui, Q., Yu, Z., Purisima, E.O., and Wang, E. (2006). Principles of microRNA regulation of a human cellular signaling network. Mol. Syst. Biol. *2*, 46.

17. Tili, E., Michaille, J.J., Gandhi, V., Plunkett, W., Sampath, D., and Calin, G.A. (2007). miRNAs and their potential for use against cancer and other diseases. Future Oncol. *3*, 521–537.

18. Ivey, K.N., Muth, A., Arnold, J., King, F.W., Yeh, R.F., Fish, J.E., Hsiao, E.C., Schwartz, R.J., Conklin, B.R., Bernstein, H.S., and Srivastava, D. (2008). MicroRNA regulation of cell lineages in mouse and human embryonic stem cells. Cell Stem Cell *2*, 219–229.

19. Wilson, K.D., Hu, S., Venkatasubrahmanyam, S., Fu, J.D., Sun, N., Abilez, O.J., Baugh, J.J., Jia, F., Ghosh, Z., Li, R.A., et al. (2010). Dynamic microRNA expression programs during cardiac differentiation of human embryonic stem cells: role for miR-499. Circ. Cardiovasc. Genet. *3*, 426–435.

20. Takaya, T., Ono, K., Kawamura, T., Takanabe, R., Kaichi, S., Morimoto, T., Wada, H., Kita, T., Shimatsu, A., and Hasegawa, K. (2009). MicroRNA-1 and microRNA-133 in spontaneous myocardial differentiation of mouse embryonic stem cells. Circ. J. *73*, 1492–1497.

21. Glass, C., and Singla, D.K. (2011). MicroRNA-1 transfected embryonic stem cells enhance cardiac myocyte differentiation and inhibit apoptosis by modulating the PTEN/Akt pathway in the infarcted heart. Am. J. Physiol. Heart Circ. Physiol. *301*, H2038–H2049.

22. Liu, N., Bezprozvannaya, S., Williams, A.H., Qi, X., Richardson, J.A., Bassel-Duby, R., and Olson, E.N. (2008). MicroRNA-133a regulates cardiomyocyte proliferation and suppresses smooth muscle gene expression in the heart. Genes Dev. *22*, 3242–3254.

23. Sharma, N.M., Nandi, S.S., Zheng, H., Mishra, P.K., and Patel, K.P. (2017). A novel role for miR-133a in centrally mediated activation of the renin-angiotensin system in congestive heart failure. Am. J. Physiol. Heart Circ. Physiol. *312*, H968–H979.

24. Porrello, E.R., Johnson, B.A., Aurora, A.B., Simpson, E., Nam, Y.J., Matkovich, S.J., Dorn, G.W., 2nd, van Rooij, E., and Olson, E.N. (2011). miR-15 family regulates postnatal mitotic arrest of cardiomyocytes. Circ. Res. *109*, 670–679.

25. Chen, J., Huang, Z.P., Seok, H.Y., Ding, J., Kataoka, M., Zhang, Z., Hu, X., Wang, G., Lin, Z., Wang, S., et al. (2013). miR-17-92 cluster is required for and sufficient to induce cardiomyocyte proliferation in postnatal and adult hearts. Circ. Res. *112*, 1557–1566.

26. Deng, S., Zhao, Q., Zhou, X., Zhang, L., Bao, L., Zhen, L., Zhang, Y., Fan, H., Liu, Z., and Yu, Z. (2016). Neonatal heart-enriched miR-708 promotes differentiation of cardiac progenitor cells in rats. Int. J. Mol. Sci. *17*, 875.

27. Zhen, L.X., Gu, Y.Y., Zhao, Q., Zhu, H.F., Lv, J.H., Li, S.J., Xu, Z., Li, L., and Yu, Z.R. (2019). miR-301a promotes embryonic stem cell differentiation to cardiomyocytes. World J. Stem Cells *11*, 1130–1141.

28. Granado, M., Amor, S., Martín-Carro, B., Guerra-Menéndez, L., Tejera-Muñoz, A., González-Hedström, D., Rubio, C., Carrascosa, J.M., and García-Villalón, Á.L. (2019). Caloric restriction attenuates aging-induced cardiac insulin resistance in male Wistar rats through activation of PI3K/Akt pathway. Nutr. Metab. Cardiovasc. Dis. *29*, 97–105.

29. Oudit, G.Y., and Penninger, J.M. (2009). Cardiac regulation by phosphoinositide 3-kinases and PTEN. Cardiovasc. Res. *82*, 250–260.

30. Lin, J., Sampath, D., Nannini, M.A., Lee, B.B., Degtyarev, M., Oeh, J., Savage, H., Guan, Z., Hong, R., Kassees, R., et al. (2013). Targeting activated Akt with GDC-0068, a novel selective Akt inhibitor that is efficacious in multiple tumor models. Clin. Cancer Res. *19*, 1760–1772.

31. Soonpaa, M.H., Kim, K.K., Pajak, L., Franklin, M., and Field, L.J. (1996). Cardiomyocyte DNA synthesis and binucleation during murine development. Am. J. Physiol. *271*, H2183–H2189.

32. Pasumarthi, K.B., and Field, L.J. (2002). Cardiomyocyte cell cycle regulation. Circ. Res. *90*, 1044–1054.

33. Kolpakov, M.A., Rafiq, K., Guo, X., Hooshdaran, B., Wang, T., Vlasenko, L., Bashkirova, Y.V., Zhang, X., Chen, X., Iftikhar, S., et al. (2016). Protease-activated receptor 4 deficiency offers cardioprotection after acute ischemia reperfusion injury. J. Mol. Cell. Cardiol. *90*, 21–29.

34. Sadahiro, T. (2019). Cardiac regeneration with pluripotent stem cell-derived cardiomyocytes and direct cardiac reprogramming. Regen. Ther. *11*, 95–100.

35. Sun, T., Dong, Y.H., Du, W., Shi, C.Y., Wang, K., Tariq, M.A., Wang, J.X., and Li, P.F. (2017). The role of microRNAs in myocardial infarction: from molecular mechanism to clinical application. Int. J. Mol. Sci. *18*, 745.

36. Huang, W., Feng, Y., Liang, J., Yu, H., Wang, C., Wang, B., Wang, M., Jiang, L., Meng, W., Cai, W., et al. (2018). Loss of microRNA-128 promotes cardiomyocyte proliferation and heart regeneration. Nat. Commun. *9*, 700.

37. Tian, Y., Liu, Y., Wang, T., Zhou, N., Kong, J., Chen, L., Snitow, M., Morley, M., Li, D., Petrenko, N., et al. (2015). A microRNA-Hippo pathway that promotes cardiomyocyte proliferation and cardiac regeneration in mice. Sci. Transl. Med. *7*, 279ra38.

38. Hu, S., Huang, M., Nguyen, P.K., Gong, Y., Li, Z., Jia, F., Lan, F., Liu, J., Nag, D., Robbins, R.C., and Wu, J.C. (2011). Novel microRNA prosurvival cocktail for improving engraftment and function of cardiac progenitor cell transplantation. Circulation *124* (11, Suppl), S27–S34.

39. McCall, M.N., Kent, O.A., Yu, J., Fox-Talbot, K., Zaiman, A.L., and Halushka, M.K. (2011). MicroRNA profiling of diverse endothelial cell types. BMC Med. Genomics *4*, 78.

40. Damodaran, C., Das, T.P., Papu John, A.M., Suman, S., Kolluru, V., Morris, T.J., Rai, S., Messer, J.C., Alatassi, H., and Ankem, M.K. (2016). miR-301a expression: a prognostic marker for prostate cancer. Urol. Oncol. *34*, 336.e13–336.e20.

41. Wang, M., Li, C., Yu, B., Su, L., Li, J., Ju, J., Yu, Y., Gu, Q., Zhu, Z., and Liu, B. (2013). Overexpressed miR-301a promotes cell proliferation and invasion by targeting RUNX3 in gastric cancer. J. Gastroenterol. *48*, 1023–1033.

42. Chen, Z., Chen, L.Y., Dai, H.Y., Wang, P., Gao, S., and Wang, K. (2012). miR-301a promotes pancreatic cancer cell proliferation by directly inhibiting Bim expression. J. Cell. Biochem. *113*, 3229–3235.

43. Zhou, P., Jiang, W., Wu, L., Chang, R., Wu, K., and Wang, Z. (2012). miR-301a is a candidate oncogene that targets the homeobox gene Gax in human hepatocellular carcinoma. Dig. Dis. Sci. *57*, 1171–1180.

44. Zhang, W., Zhang, T., Jin, R., Zhao, H., Hu, J., Feng, B., Zang, L., Zheng, M., and Wang, M. (2014). MicroRNA-301a promotes migration and invasion by targeting TGFBR2 in human colorectal cancer. J. Exp. Clin. Cancer Res. *33*, 113.

45. Sansal, I., and Sellers, W.R. (2004). The biology and clinical relevance of the PTEN tumor suppressor pathway. J. Clin. Oncol. *22*, 2954–2963.

46. Lu, X.X., Cao, L.Y., Chen, X., Xiao, J., Zou, Y., and Chen, Q. (2016). *PTEN* inhibits cell proliferation, promotes cell apoptosis, and induces cell cycle arrest via downregulating the PI3K/AKT/*hTERT* pathway in lung adenocarcinoma A549 Cells. BioMed Res. Int. *2016*, 2476842.

47. Du, Y., Liu, P., Chen, Z., He, Y., Zhang, B., Dai, G., Xia, W., Liu, Y., and Chen, X. (2019). PTEN improve renal fibrosis in vitro and in vivo through inhibiting FAK/AKT signaling pathway. J. Cell. Biochem. *120*, 17887–17897.

48. Ebbesen, S.H., Scaltriti, M., Bialucha, C.U., Morse, N., Kastenhuber, E.R., Wen, H.Y., Dow, L.E., Baselga, J., and Lowe, S.W. (2016). Pten loss promotes MAPK pathway dependency in HER2/neu breast carcinomas. Proc. Natl. Acad. Sci. USA *113*, 3030–3035.

49. Sun, H., Lesche, R., Li, D.M., Liliental, J., Zhang, H., Gao, J., Gavrilova, N., Mueller, B., Liu, X., and Wu, H. (1999). PTEN modulates cell cycle progression and cell survival by regulating phosphatidylinositol 3,4,5,-trisphosphate and Akt/protein kinase B signaling pathway. Proc. Natl. Acad. Sci. USA *96*, 6199–6204.

50. Liu, L., Zhao, X., Pierre, S.V., and Askari, A. (2007). Association of PI3K-Akt signaling pathway with digitalis-induced hypertrophy of cardiac myocytes. Am. J. Physiol. Cell Physiol. *293*, C1489–C1497.

51. Jennings, R.B. (2013). Historical perspective on the pathology of myocardial ischemia/reperfusion injury. Circ. Res. *113*, 428–438.

52. Xu, J., Tang, Y., Bei, Y., Ding, S., Che, L., Yao, J., Wang, H., Lv, D., and Xiao, J. (2016). miR-19b attenuates H_2O_2-induced apoptosis in rat H9C2 cardiomyocytes via targeting PTEN. Oncotarget *7*, 10870–10878.